33rd Annual International Conference of the IEEE EMBS
Boston, Massachusetts USA, August 30 - September 3, 2011

Analysis of Local Field Potential Signals: A Systems Approach

David Huberdeau; Harrison Walker; He Huang; Erwin Montgomery; Sridevi V. Sarma, IEEE Member

Abstract— **Efficient methods for Local Field Potential (LFP) signal analysis amenable to interpretation are becoming increasingly relevant. LFP signals are believed, in part, to reflect neural action potential activity, and LFP frequency modulations are linked to spiking events. Furthermore, LFP signals are increasingly accessible in human brain regions previously unreachable due to a proliferation of deep brain stimulation implantation procedures. Traditional LFP analysis involves computing power spectra densities (PSDs) of these signals, which captures power at various frequencies in the signal. However, PSDs are second order statistics and may not capture non-trivial temporal dependencies that exist in the raw data. In this paper, we propose an LFP analysis method that is useful for describing unique features of temporal dependencies in LFP signals. This method is based on autoregressive (AR) modeling and draws from the systems identification sub-field of systems and control. Specifically, we have built and analysed AR models of LFP activity, and have demonstrated statistically significant differences in temporal dependencies between diseased globus pallidus tissue and control regions in two dystonia patients receiving deep brain stimulation implantation. Differences in the PSDs of LFP signals between these two groups were not statistically significant.**

I. INTRODUCTION

Local Field Potential (LFP) signals are a type of neural signal obtained from micro- or macro- electrode recordings from the cortex or other brain regions. Although precise characterization of the origination of LFP signals is still debated, evidence indicates that LFP activity (e.g. oscillations) are coupled with neuronal discharge events [2], [3], [4]. A combination of greater ease of access to LFP signals via macro-electrode recordings during neurosurgery [1], [3], [6], [4], [7] and evidence of correlation of LFP signals with neuronal spiking [5], [7] creates a need for improved and/or alternative LFP analysis methods.

Existing LFP signal analysis methods have mainly relied on computations in the frequency domain, such as power spectra density, cross-spectra density, and coherence [1], [3], [4], [8], [7], [9], [10]. These methods are generally reliable for determining the frequency content of LFP signals, and subsequently studying characteristics of the neural system being probed, including the information content of the LFP signal at various frequencies, how the neural system is related to other brain areas, and how the LFP signal is related to other neural signals [1], [3], [4], [8], [7], [9], [10]. However, these methods have inherent limitations due to the non-stationary nature of or temporal dependencies in the LFP signals ([8], [10]). They also fail to characterize other relevant properties of the neural systems, including causality, stability, and levels of amplification provided by the neural circuit on the LFP signals. Precise definitions of these characteristics are provided later. Finally, these statistics are purely descriptive, and make no headway towards predictive models which may have advantages when engineering improved therapeutics.

The method of LFP analysis proposed herein employs autoregressive (AR) modeling and standard techniques from the systems identification field. AR modeling is a method of curve fitting for random processes. The simplest AR models relate past events in a linear difference equation to predict future events. The method estimates an AR model for each LFP signal and then represents the model with a state space description (see Deistler for review paper [11]). The state space description entails a state evolution equation and an output equation. The state evolution equation provides information about system stability and temporal dependence in the maximum eigenvalue and the maximum singular value, respectively.

This method of analysis provides insights that may be unattainable with PSD-based computations alone. We support this assertion with novel results presented below. We have applied this analysis method to LFP signals acquired during implantation of deep brain stimulation electrodes in two human dystonia patients. LFP signals acquired from affected brain regions were compared to LFP signals acquired from unaffected brain regions. PSDs of these signals showed no statistically significant differences between the two groups. However, the method proposed here showed that LFP activity in unaffacted regions had significantly greater temporal dependencies (i.e. memory) than affected regions. Our findings suggest that GPi regions associated with affected body regions lose their ability to retain information (i.e. lose memory) and generate neural signals that are closer to white noise, which may cause the observed movement disorders in patients.

II. METHODS

Here, we model the LFP activity as the output of a linear time invariant system driven by white Gaussian noise. The model structure belongs to the well known autoregressive (AR) class. We then describe the state space representation of such models and summarize the measures from a state space model that we use to analyse LFP data.

This work was supported by the Burroughs Wellcome Fund CASI Grant (Sridevi Sarma)

Sridevi Sarma and David Huberdeau are with the Dept. of Biomedical Engineering, Johns Hopkins University, 3400 N. Charles St., Baltimore, MD 21218, USA ssarma2@jhu.edu, dhuberd1@jhu.edu, respectively

Erwin Montgomery , Harrison Walker, and He Huang are with the Dept. of Neuroscience, University of Alabama, SC 360A, 1720 7th Ave S, Birmingham AL 35294-0017 emontgom@uab.edu

A. AR Models of LFP Signals

Our approach to analysing LFP signals is to compute and analyse AR models. In particular, we assume that the LFP signal at discrete time bin k, denoted as y_k, is the output of a linear system driven by white Gausssian noise, n_k. The linear model is described by the following input-output difference equation:

$$y_k = \sum_{i=1}^{n} \alpha_i y_{k-i} + \eta_k \tag{1}$$

where y_k is a random process indexed by k, n is the model order, α_i (for $i \in \{1, ..., n\}$) are model parameters, and η_k is additive zero mean white Gaussian noise (error term).

Many methods exist for estimating the model parameters α_i. We use the least squares algorithm to estimate the parameters on training data and then measure goodness-of-fit on separate test data. In particular, we use the training data of length N to define

$$\mathbf{y} = \begin{bmatrix} y_n & y_{n+1} & \cdots & y_N \end{bmatrix}^T$$

$$\mathbf{A} = \begin{bmatrix} y_{n-1} & y_{n-2} & \cdots & y_0 \\ y_n & y_{n-1} & \cdots & y_1 \\ \vdots & & \vdots & \\ y_{N-1} & y_{N-2} & \cdots & y_{N-n} \end{bmatrix} \tag{2}$$

$$\alpha = \begin{bmatrix} \alpha_1 & \alpha_2 & \cdots & \alpha_n \end{bmatrix}^T$$

$$\eta = \begin{bmatrix} \eta_n & \eta_{n+1} & \cdots & \eta_N \end{bmatrix}^T$$

and minimize $||\mathbf{A}\alpha - \mathbf{y}||_2$. Since the additive noise term is Gaussian, minimizing the least squared error is equivalent to maximizing the likelihood function [12].

Once the model parameters are estimated, test data is used to validate the model. Model fit is quantified by calculating the normalized 2-norm of the model residual, defined as $[modelfit] = \frac{||residuals||_2}{||signal||_2}$. The normalized residuals provides a measure of the relative amount that the predicted LFP signal deviates from the actual LFP signal.

B. State Space Representation

AR model parameters by themselves can provide information related to the temporal dependencies in the LFP data. In particular, the 2-norm of the parameter vector gives a notion of the amount of such dependencies or "memory" in LFP activity. The larger $||\alpha||_2$ indicates more dependency on past values of LFP activity. That is, at some time k, y_k strongly depends on previous values. However, in this analysis, we analyse the LFP activity by first constructring the equivalent state space representation of the AR model.

We define the state vector at time k as

$$\mathbf{x_k} = \begin{bmatrix} y_{k-1} & y_{k-2} & \cdots & y_{k-n} \end{bmatrix}^T$$

TABLE I

STATE SPACE SYSTEM FEATURES

Model Feature:	**Symbol:**	**Explanation:**
Maximum eigenvalue of A	$max(\|\lambda\{A\}\|)$	System with any eigenvalue magnitude greater than 1 is not asymptotically stable
Maximum singular value of A	$\sigma_{max}\{A\}$	The amount of temporal dependency in the output signal
Minimum singular value of A	$\sigma_{min}\{A\}$	Indicates the smallest additive perturbation that will make the matrix A singular
Ratio: Maximum singular value of A to minimum singular value of A	$\frac{\sigma_{max}\{A\}}{\sigma_{min}\{A\}}$	This ratio indicates dominant modes of the system

Then the state space representation is:

$$\begin{aligned} \mathbf{x_{k+1}} &= A\mathbf{x_k} + B\eta_k \\ y_k &= C\mathbf{x_k} + D\eta_k \end{aligned} \tag{3}$$

where

$$A = \begin{bmatrix} \alpha_1 & \alpha_2 & \cdots & \alpha_n \\ 1 & \cdots & 0 & 0 \\ \vdots & \ddots & \vdots & \vdots \\ 0 & \cdots & 1 & 0 \end{bmatrix}$$

$$B = \begin{bmatrix} 1 & 0 & \cdots & 0 \end{bmatrix}^T$$

$$C = \begin{bmatrix} \alpha_1 & \alpha_2 & \cdots & \alpha_n \end{bmatrix}$$

$$D = 1$$

Equation 3 defines the state space difference equation. It describes how the output y_k is related to the states $\mathbf{x}$ and the random noise η through a linear equation, and how $\mathbf{x}$ evolves over time.

Modeling a process as a linear dynamical system in state space form opens up new avenues of analysis. Among these, computations performed on the state evolution matrix A reveals important properties of the system model, including stability, maximum amplification, and sensitivity to perturbations. Table I lists the computations that may be performed on the matrix A and what each represents.

We note that the maximum singular value indicates the level of memory in the LFP acitivty as it is straightforward to show that

$$\sigma_{max}^2 - 1 \leq ||\alpha||_2^2 \leq \sigma_{max}^2 \tag{4}$$

III. RESULTS

We apply our method to LFP signals recorded from the globus pallidus internus (GPi) segments in two patients with generalized dystonia. Generalized dystonia is a movement disorder characterized by sustained involuntary muscle contractions that can lead to severe disability [13]. We focus

our attention here to manifestations of dystonia in patients with no clear confounding co-morbidities. Our aim is to find quantifiable differences between neural signals originating from unaffected GPi regions (regions in the GPi homunculus that correspond to body parts that are not impacted by the disease), and those that originate from affected GPi regions of patients. We also compute standard PSDs to show that these traditional measures do not show statistically significant differences between the two groups studied.

A. Patients and Recordings

Two dystonia patients with idiopathic cervical dystonia (abreviated TR and KW) received implantation of deep brain stimulation electrodes in the globus pallidus internal (GPi) segment in accordance with standard surgical procedures [14]. LFP signals were obtained from microelectrode recordings (microTargeting^{TM}mT Electrodes, FHC Inc., Bowdoin, ME, USA) during deep brain stimulation electrode implantation. In all, there were 13 usable single-channel trials from each patient, with average trial duration of 124-s (max/min duration: 128/122-s). Simultaneous single unit spiking activity was also recorded, but is not included in this analysis. Electrode placement within the GPi was verified by monitoring single-unit activity during electrode advancement. Classification of each recording sight as being "affected" or "unaffected" was accomplished by identifying the functional area (e.g. hand, wrist, etc.) associated with each recording, and noting the presence or absence of dystonic symptoms. A table summarizing the functional region and affectedness state associated with each recording trial is provided in table II.

Trials consisted of simple rest periods; though, both patients exhibited active dystonic symptoms within trials, which included involuntary muscle contractions. LFP signals were sampled at 25-kHz using (National Instruments DAQ-6014 16bits A/D converter, National Instruments Co., Austin, TX, USA), amplified by 10,000 and band-pass filtered between 10-Hz and 10-kHz before being saved to file for post-processing.

TABLE II
PATIENT INFORMATION AND ELECTRODE PLACEMENT

	Patient TR		**Patient KW**	
	Recording		**Recording**	
Trial No.	**Gpi Region**	**Affected**	**Gpi Region**	**Affected**
1	Ankle	NO	Knee	NO
2	Ankle	NO	Wrist	NO
3	Ankle	NO	Wrist	NO
4	Ankle	NO	Elbow	NO
5	Jaw	YES	Wrist	NO
6	Tongue	YES	Head	YES
7	Tongue	YES	Head	YES
8	Head	YES	Head	YES
9	Head	YES	Head	YES
10	Head	YES	Head	YES
11	Knee	NO	Head	YES
12	Ankle	NO	Head	YES
13	Ankle	NO	Head	YES

Table II provides the GPi recording region and affectedness state for each trial number for patients TR and KW.

B. AR Model Estimation

Discrete LFP signals were processed in Matlab 2008a (The Mathworks, Cambridge, MA) using the signal processing toolbox and custom software. PSD plots were created for the purposes of comparison of the AR method with a more standard method. For the PSD computations, each trial was separated into 1-s non-overlapping segments, and computation of the Fourier transform-based PSD was applied over all segments using a rectangular window. This level of segmentation was chosen in an attempt to mitigate effects of high frequency noise in the LFP signals, while balancing the need for adequate frequency resolution.

To compute AR models, all 13 discrete LFP signals for each patient were digitally filtered using a moving-average decimation algorithm, implemented with a 250-order Finite Impulse Response (FIR) filter, which down-sampled the LFP data to 100-Hz. Each filtered signal was then separated into 25-s segments, each of which was further partitioned into training and testing data vectors, with the leading 80% of the contiguous signal flagged as train and the trailing 20% flagged as testing.

Normalized residual 2-norm values were computed to assess model fit for each AR model using each 25-s segment of test data for each patient. Those models which provided the most significant results (shown later) were models of order seven and had mean normalized residuals of 0.147 for patient TR and 0.226 for patient KW. We believe this magnitude of error is acceptable for this analysis.

C. AR Model Features

We computed each of the system features listed in Table I for every 25-s segment of FIR-filtered LFP data, and for each model order $n = \{1, \cdots, n\}$. The model feature with the most significant difference between affected and unaffected regions for both patients was the maximum singular value. This is indicated by difference-in-means, non-equal variance t-tests performed between affected and unaffected feature computations.

Figure 1 provides a visual representation of the maximum singular value computation results for the best performing model for both patients. This figure highlights the difference in feature values between affected and unaffected GPi regions, for models of order seven.

The other model features do not provide the same level of difference between the affectedness states in these patients.

D. PSD Computations

Figure 2 shows the PSD plots of LFP signals. This analysis was included to show the lack of progress in correctly classifying LFP signals from GPi recording sights as being either affected or unaffected on second-order statistics (the PSD) alone. (A) and (B) display the mean power density (solid line and 95% confidence bounds) across all 1-s LFP segments recorded from un-affected GPi sites, averaged within frequency bands. (C) and (D) show the same for

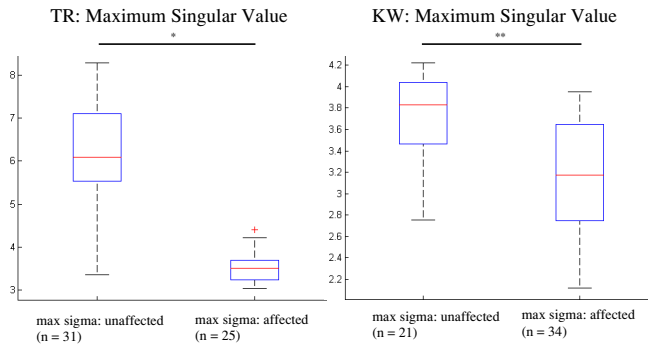

Fig. 1. **Maximum Singular Value** - Stem and leaf plot of the maximum singular value computations for AR models of order 7 for each patient. *p-value = 1.95E-12. **p-value = 5.97E-5

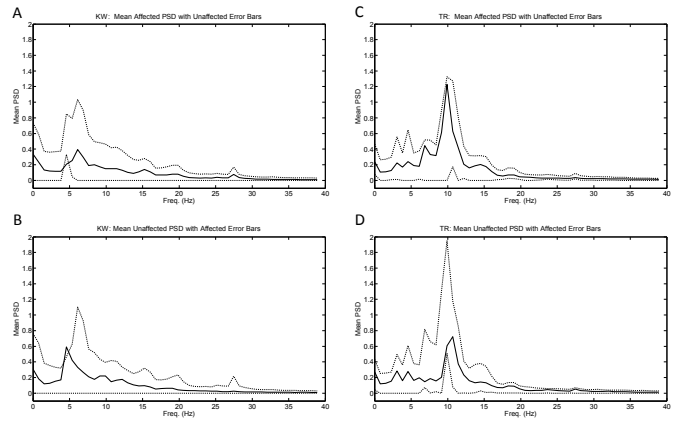

Fig. 2. **Power Spectral Densities** - Mean PSD plots (solid lines), averaged within frequency bands, for both TR (A, B) and for KW (C, D). 95% error bounds (dashed lines) computed from data of the opposite affectedness state are displayed concurrently to illustrate the lack of statistically significant difference between affected and unaffected GPi regions.

recordings in affected GPi sites. Although noticeable differences exist between patients, the statistical aggregate spectra do not significantly differ between affected and unaffected regions within patients.

IV. Discussion

AR modeling is widely used in several domains. Cassidy, et. al. employed a variation of the method proposed here, but chose a different route for analysis [10]. They used dynamic multivariate autoregressive (MAR) models to investigate the non-stationary coherence among LFP signals in the STN and GPi, and with electroencephalography (EEG) signals.

We have taken that analysis in a different direction by producing state space system representations of the AR models and analysing the transition matrix properties in the state evolution equation. As seen above, the maximum singular value feature of the AR-based state space models depict the most significant difference between unaffected and affected GPi regions, indicating that the $\max(\sigma(A))$ may have broader underlying meaning in the context of LFP analysis. In system's theory, $\max(\sigma(A))$ indicates the level of temporal dependencies in the data.

Could this mean that the response of the GPi on LFP signals is muted in regions corresponding to muscle groups afflicted with dystonia or that the neural circuit loses memory in afflicted regions? To better decipher the system's response characteristics, it is necessary to control the input signal by way of modulating LFP activity within the GPi. However, due to limitations on intra-surgical experimentation methods, we were unable to generate the system input stimulus required to build more complicated models.

V. Acknowledgments

The authors gratefully acknowledge reviewers' comments and the entire Sarma Lab and Montgomery Lab.

References

[1] Peter Brown, Antonio Oliviero, Paolo Mazzone, Angelo Insola, Pietro Tonali, and Vincenzo Di Lazzaro. *Dopamine Dependency of Oscillations between Subthalamic Nucleus and Pallidum in Parkinson's Disease.* The Journal of Neuroscience, 1 February 2001, 21(3): 1033-1038.

[2] Creutzfeldt, O.D.; Watanabe, S.; Lux, H.D. *Relations Between EEG and Phenomena and Potentials of Single Cortical Cells. I. Evoked Responses After Thalamic and Epicotrical Stimulation.* Electroencephalography and Clinical Neurophysiology. 1966. 20: 1-18.

[3] Andrea A. Khn, Thomas Trottenberg, Anatol Kivi, Andreas Kupsch, Gerd-Helge Schneider, and Peter Brown. *The relationship between local field potential and neuronal discharge in the subthalamic nucleus of patients with Parkinson's disease.* Experimental Neurology. Volume 194, Issue 1, July 2005, Pages 212-220.

[4] Levy R, Ashby P, Hutchison WD, Lang AE, Lozano AM, Dostrovsky JO. *Dependence of subthalamic nucleus oscillations on movement and dopamine in Parkinsons disease.* Brain 2002;125:11961209.

[5] Jeremy R.Manning, Joshua Jacobs, Itzhak Fried and Michael J. Kahana. *Broadband Shifts in Local Field Potential Power Spectra Are Correlated with Single-Neuron Spiking in Humans.* The Journal of Neuroscience, October 28, 2009. 29(43):1361313620

[6] Peter Brown. *Oscillatory Nature of Human Basal Ganglia Activity: Relationship to the Pathophysiology of Parkinsons Disease.* Movement Disorders. Vol. 18, No. 4, 2003, pp. 357363.

[7] Paul Silberstein, Andrea A. Kuhn, Andreas Kupsch, Thomas Trottenberg, Joachim K. Krauss, Johannes C. Wohrle, Paolo Mazzone, Angelo Insola, Vincenzo Di Lazzaro, Antonio Oliviero, Tipu Aziz, and Peter Brown. *Patterning of globus pallidus local field potentials differs between Parkinson's disease and dystonia.* Brain (2003), 126, 25972608.

[8] B. Masimore , J. Kakalios , A.D. Redish. *Measuring fundamental frequencies in local field potentials.* Journal of Neuroscience Methods. 138 (2004) 97105.

[9] Williams, D.; Tijssen, M; van Bruggen, G.; Bosch, A.; Insola, A; Di Lazzaro, V.; Mazzone, P.; Oliviero, A.; Quartarone, A.; Speelman, H.; Brown, P. *Dopamine-dependent changes in the functional connectivity between basal ganglia and cerebral cortex in humans.* Brain 2002, 125, 1558 69.

[10] Cassidy, M.; Mazzone, P.; Oliviero, A.; Insola, A.; Pietro, T.; Di Lazzaro, V.; Brown, P. *Movement-Related Changes in Synchronization in the Human Basal Ganglia.* Brain 2002, 125: 1235 - 46.

[11] Deistler, M. *System Identification and Time Series Analysis: Past, Present, and Future.* Stochastic Theory and Control, LNCIS 280, pp. 97109, 2002.

[12] Lhung, Lennart. *System Identification: Theory for the User, 2nd ed.* Upper Saddle River, NJ. Prentice Hall, 1999.

[13] Nemeth, Andrea. "Dystonia Overview" in *Gene Reviews*. Seattle, WA. University of Washington, 1993.

[14] Marie Vidailhet, David Grabli, and Emmanuel Roze. *Deep Brain Stimulation in Dystonia.* Current Clinical Neurology: Deep Brain Stimulation in Neurological and Psychiatric Disorders, 2008. Humana Press, Totowa, NJ.